Laplace-Domain Solutions for Radial Two-Zone Flow Equations under the Conditions of Constant-Head and Partially Penetrating Well

Shaw-Yang Yang[1] and Hund-Der Yeh[2]

Abstract: A mathematical model is presented for a constant-head test performed in a partially penetrating well with a finite-thickness skin. The model uses a no-flow boundary condition for the casing and a constant-head boundary condition for the screen to represent the partially penetrating well. The Laplace-domain solutions for the dimensionless flow rate at the wellbore and the hydraulic heads in the skin and formation zones are derived using the Laplace and finite Fourier cosine transforms. The solutions of hydraulic heads have been shown to satisfy the governing equations, related boundary conditions, and continuity requirements for the pressure head and flow rate at the interface of the skin zone and undisturbed formation. In addition, an efficient algorithm for evaluating those solutions is also presented. The dimensionless flow rates obtained from new solutions have been shown to be better than those of Novakowski's solutions, especially when the penetration ratio is large.

DOI: 10.1061/(ASCE)0733-9429(2005)131:3(209)

CE Database subject headings: Ground water; Mathematical models; Thickness; Wells.

Introduction

The constant-flux and constant-head tests are two typical kinds of aquifer tests. The former is required to maintain a constant well discharge (or injection) and measure the drawdowns at the observation wells. The latter, frequently employed in engineering practice for low permeability aquifers, is carried out in a single well, which maintains a constant water level inside the well and measures the transient flow rate at the wellbore. A patchy aquifer with a well centered in a uniform disk of transmissivity T_1 embedded within a formation of transmissivity T_2 can be considered as a radial two-zone system. In addition, an aquifer may also be considered as a two-zone system if the formation properties near the wellbore are significantly changed due to well construction and/or development. The drilling process may produce a positive wellbore skin that has lower permeability than the undisturbed formation. Conversely, thorough well development removes fine particles from the surrounding formation and produces a negative wellbore skin with an increased permeability. In fact, the positive wellbore skin prevails under most field conditions (Novakowski 1989).

Two types of skins, the infinitesimal and finite-thickness skins, were used in the past to investigate the skin effect on the results of constant-head tests. Streltsova and McKinley (1984) considered an infinitesimal skin and used a skin factor to stand for the skin effect. Chang and Chen (1999) gave the Laplace-domain solutions of hydraulic heads and flow rates for a confined aquifer under the effects of finite-thickness skin and fully penetrating well. They presented curves representing specific capacity versus time to investigate the influence of low-permeability skin zone on the estimation of aquifer parameters. Yang and Yeh (2002) obtained the time-domain solution for the wellbore flow rate by using the Laplace transforms and the Bromwich integral method. Considering the effects of finite-thickness skin and well partial penetration, Novakowski (1993) derived a Laplace-domain solution for dimensionless transient flow rate at the wellbore. Curves of dimensionless flow rate versus dimensionless time were developed to investigate the influences of finite-thickness skin and well partial penetration. Markle et al. (1995) developed a model for a partially penetrating well that has a finite-thickness skin and intersects a single vertical fracture. Their results show that the finite-thickness skin and partially penetrating well can affect the transient flow rate at the wellbore. For a mixed boundary value problem, Cassiani et al. (1999) developed a new semianalytic solution for a partially penetrating well with infinitesimal skin situated in an anisotropic confined aquifer. They employed a no-flow boundary condition along the casing and a third-type boundary condition by specifying the drawdown due to pumping and skin effect along the well screen. Their solution is suitable to aquifers having a semi-infinite vertical extent or to packer tests with aquifer horizontal boundaries far enough from the tested area. Chang and Chen (2002) used the same mathematical model as Cassiani et al. (1999) except that the aquifer thickness is finite and the flux entering through the well screen is a function of time and location along the screen. Their solution includes a rigorous treatment of the boundary condition at the wellbore. However, the accuracy of their solution may depend on the number of segments chosen for representing the screen length.

A mathematical model describing the constant-head test per-

[1]Associate Professor Dept. of Civil Engineering, Vanung Univ. Chungli, Taiwan.

[2]Professor, Institute of Environmental Engineering, National Chiao Tung Univ. Hsinchu, Taiwan (corresponding author). E-mail: hdyeh@mail.nctu.edu.tw

Note. Discussion open until August 1, 2005. Separate discussions must be submitted for individual papers. To extend the closing date by one month, a written request must be filed with the ASCE Managing Editor. The manuscript for this paper was submitted for review and possible publication on February 11, 2004; approved on August 18, 2004. This paper is part of the ***Journal of Hydraulic Engineering***, Vol. 131, No. 3, March 1, 2005. ©ASCE, ISSN 0733-9429/2005/3-209–216/ $25.00.

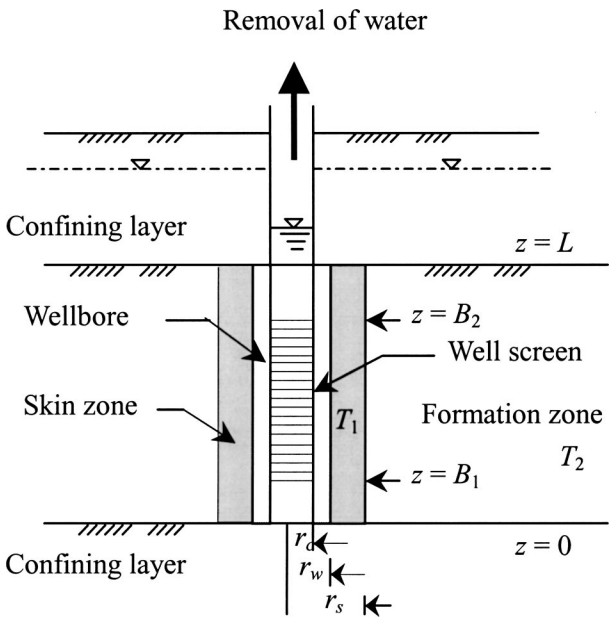

Fig. 1. Schematic diagram of the well and aquifer configurations

formed in a radial confined aquifer system with the finite-thickness skin and partially penetrating well is presented. The model uses a no-flow boundary condition for the casing and constant-head boundary condition for the screen to represent a partially penetrating well. The Laplace-domain solutions for the model are derived using the Laplace and finite Fourier cosine transforms. An efficient numerical approach, including the modified Crump method, for performing the numerical Laplace inversion and the Shanks method for accelerating convergence when evaluating the sum of terms and the Bessel functions, is also proposed. Those solutions can be employed to predict the hydraulic head in the aquifer and transient flow rate at the wellbore, to explore the effects of the finite-thickness skin and well partial penetration on the hydraulic heads and transient flow rates, and to identify the hydraulic parameters in aquifer data analyses.

Mathematical Model

Mathematical Statement

Fig. 1 is a cross-sectional view of confined aquifer system with a well under the conditions of partial penetration and finite-thickness skin. The system assumes: (1) The aquifer is homogeneous, infinite extent, and with a constant thickness; (2) the well has a finite radius; and (3) the initial head is constant and uniform throughout the whole aquifer. Under these assumptions, the governing equations for hydraulic head distributions in the skin and formation zones can, respectively, be written as

$$K_{r1}\frac{\partial^2 H_1}{\partial r^2}+\frac{K_{r1}}{r}\frac{\partial H_1}{\partial r}+K_{z1}\frac{\partial^2 H_1}{\partial z^2}=S_{s1}\frac{\partial H_1}{\partial t},\quad r_w\leqslant r\leqslant r_s \tag{1}$$

and

$$K_{r2}\frac{\partial^2 H_2}{\partial r^2}+\frac{K_{r2}}{r}\frac{\partial H_2}{\partial r}+K_{z2}\frac{\partial^2 H_2}{\partial z^2}=S_{s2}\frac{\partial H_2}{\partial t},\quad r_s\leqslant r<\infty \tag{2}$$

where the subscripts 1 and 2, respectively, denote the skin and formation zones; H [or $H(r,z,t)$]=hydraulic head; r=radial distance from the centerline of well; r_w=well radius; r_s=radial distance from the well centerline to the outer skin envelope; t=time from the start of test; K_r=hydraulic conductivity in a radial direction; K_z=hydraulic conductivity in a vertical direction; and S_s=specific storativity.

The hydraulic heads are initially assumed to be zero within the well and the skin and formation zones, that is

$$H_1(r,z,0)=H_2(r,z,0)=0,\ r\geqslant r_w \tag{3}$$

When $r=r_w$, the hydraulic head represents the well water level if the well loss is negligible.

When r approaches infinity, the boundary condition for the formation zone gives

$$H_2(\infty,z,t)=0 \tag{4}$$

The continuities of hydraulic head and flow rate at the interface of the skin and formation zones, respectively, require

$$H_1(r_s,z,t)=H_2(r_s,z,t),\quad t>0 \tag{5}$$

and

$$K_{r1}\frac{\partial H_1(r_s,z,t)}{\partial r}=K_{r2}\frac{\partial H_2(r_s,z,t)}{\partial r},\quad t>0 \tag{6}$$

The no-flow boundary conditions at the bottom and upper impervious boundaries of confined aquifer are, respectively,

$$\frac{\partial H_1(r,0,t)}{\partial z}=\frac{\partial H_2(r,0,t)}{\partial z}=0 \tag{7}$$

and

$$\frac{\partial H_1(r,L,t)}{\partial z}=\frac{\partial H_2(r,L,t)}{\partial z}=0 \tag{8}$$

The water level of well remains constant at $r=r_w$. Thus, the inner boundary condition specified along the wellbore is

$$H_1(r_w,z,t)=H_0\delta(z-z') \tag{9}$$

where H_0=constant water level around the well at any time; $\delta(\cdot)$=Dirac delta function; and z'=location of point source in a z direction.

The flow rate along the screen assumes that

$$-K_{r1}\frac{\partial H_1(r_w,z,t)}{\partial r}=q(t),\quad B_1\leqslant z\leqslant B_2 \tag{10}$$

and the no-flow boundary condition along the well casing is

$$-K_{r1}\frac{\partial H_1(r_w,z,t)}{\partial r}=0,\quad z<B_1,\quad z>B_2 \tag{11}$$

where $q(t)$=flow rate per unit area and assumed constant along the well screen; and B_1 and B_2=lower and upper z coordinates, respectively.

The dimensionless parameters used hereafter are defined in Table 1. Eqs. (1)–(11) in dimensionless form are, respectively,

$$\frac{\partial^2 h_1}{\partial r_D^2}+\frac{1}{r_D}\frac{\partial h_1}{\partial r_D}+\alpha_1\frac{\partial^2 h_1}{\partial z_D^2}=\gamma\xi\frac{\partial h_1}{\partial\tau},\quad 1\leqslant r_D\leqslant r_{Ds} \tag{12}$$

$$\frac{\partial^2 h_2}{\partial r_D^2}+\frac{1}{r_D}\frac{\partial h_2}{\partial r_D}+\alpha_2\frac{\partial^2 h_2}{\partial z_D^2}=\frac{\partial h_2}{\partial\tau},\quad r_{Ds}\leqslant r_D<\infty \tag{13}$$

$$h_1(r_D,z_D,0)=h_2(r_D,z_D,0)=0 \tag{14}$$

J. Hydraul. Eng. 2005.131:209-216.

Table 1. Dimensionless Expressions

Symbol	Illustration
τ	$K_{r2}t/S_{s2}r_w^2$
r_{Ds}	r_s/r_w
r_D	r/r_w
L_D	L/r_w
h_1	H_1/H_0
h_2	H_2/H_0
z_D	z/r_w
b_1	B_1/r_w
b_2	B_2/r_w
ϕ	$(B_2-B_1)/L$
α_1	K_{z1}/K_{r1}
α_2	K_{z2}/K_{r2}
γ	K_{r2}/K_{r1}
ξ	S_{s1}/S_{s2}
$q_D(\tau)$	$q(t)/[2\pi(B_2-B_1)K_{r1}H_0]$
q_1	$\sqrt{\alpha_1 w_n^2+\gamma\xi p}$
q_2	$\sqrt{\alpha_2 w_n^2+p}$
q_3	$\sqrt{\gamma\xi p}$
q_4,q'	$\sqrt{p}$
β_1	$-q_1K_1(q_1r_{Ds})K_0(q_2r_{Ds})+\gamma q_2K_0(q_1r_{Ds})K_1(q_2r_{Ds})$
β_2	$q_1I_1(q_1r_{Ds})K_0(q_2r_{Ds})+\gamma q_2I_0(q_1r_{Ds})K_1(q_2r_{Ds})$
β_3	$-q_3K_1(q_3r_{Ds})K_0(q_4r_{Ds})+\gamma q_4K_0(q_3r_{Ds})K_1(q_4r_{Ds})$
β_4	$q_3I_1(q_3r_{Ds})K_0(q_4r_{Ds})+\gamma q_4I_0(q_3r_{Ds})K_1(q_4r_{Ds})$
$A_1(r_D)$	$[-\beta_3I_0(q_3r_D)+\beta_4K_0(q_3r_D)]/\{q_3[\beta_3I_1(q_3)+\beta_4K_1(q_3)]\}$
$A_2(r_D)$	$[-\beta_1I_0(q_1r_D)+\beta_2K_0(q_1r_D)]/\{q_1[\beta_1I_1(q_1)+\beta_2K_1(q_1)]\}$
$A_3(w_n)$	$[\sin(w_nb_2)-\sin(w_nb_1)]/w_n$
$B_1(r_D)$	$K_0(q_4r_D)/\{q_3r_{Ds}[\beta_3I_1(q_3)+\beta_4K_1(q_3)]\}$
$B_2(r_D)$	$K_0(q_2r_D)/\{q_1r_{Ds}[\beta_1I_1(q_1)+\beta_2K_1(q_1)]\}$
$A_1(r_D=1)$	$[-\beta_3I_0(q_3)+\beta_4K_0(q_3)]/\{q_3[\beta_3I_1(q_3)+\beta_4K_1(q_3)]\}$
$A_2(r_D=1)$	$[-\beta_1I_0(q_1)+\beta_2K_0(q_1)]/\{q_1[\beta_1I_1(q_1)+\beta_2K_1(q_1)]\}$

$$h_2(\infty,z_D,\tau)=0 \tag{15}$$

$$h_1(r_{Ds},z_D,\tau)=h_2(r_{Ds},z_D,\tau),\quad \tau>0 \tag{16}$$

$$\frac{\partial h_1(r_{Ds},z_D,\tau)}{\partial r_D}=\gamma\frac{\partial h_2(r_{Ds},z_D,\tau)}{\partial r_D},\quad \tau>0 \tag{17}$$

$$\frac{\partial h_1(r_D,0,\tau)}{\partial z_D}=\frac{\partial h_2(r_D,0,\tau)}{\partial z_D}=0 \tag{18}$$

$$\frac{\partial h_1(r_D,L_D,\tau)}{\partial z_D}=\frac{\partial h_2(r_D,L_D,\tau)}{\partial z_D}=0 \tag{19}$$

$$h_1(1,z_D,\tau)=\delta(z_D-z_D') \tag{20}$$

$$-\frac{\partial h_1(1,z_D,\tau)}{\partial r_D}=q_D(\tau),\quad b_1\leq z_D\leq b_2 \tag{21}$$

and

$$-\frac{\partial h_1(1,z_D,\tau)}{\partial r_D}=0,\quad z_D<b_1,\quad z_D>b_2 \tag{22}$$

Laplace-Domain Solutions

The Laplace-domain solution for dimensionless hydraulic heads in the skin and formation zones can be obtained by taking Laplace transforms with respect to time and the finite Fourier cosine transforms with respect to z coordinate from Eqs. (12)–(22). Taking the Laplace transforms of Eqs. (12)–(22) yields

$$\frac{\partial^2\tilde{h}_1}{\partial r_D^2}+\frac{1}{r_D}\frac{\partial\tilde{h}_1}{\partial r_D}+\alpha_1\frac{\partial^2\tilde{h}_1}{\partial z_D^2}=\gamma\xi p\tilde{h}_1,\quad 1\leq r_D\leq r_{Ds} \tag{23}$$

$$\frac{\partial^2\tilde{h}_2}{\partial r_D^2}+\frac{1}{r_D}\frac{\partial\tilde{h}_2}{\partial r_D}+\alpha_2\frac{\partial^2\tilde{h}_2}{\partial z_D^2}=p\tilde{h}_2,\quad r_{Ds}\leq r_D<\infty \tag{24}$$

$$\tilde{h}_2(\infty,z_D,p)=0 \tag{25}$$

$$\tilde{h}_1(r_{Ds},z_D,p)=\tilde{h}_2(r_{Ds},z_D,p) \tag{26}$$

$$\frac{\partial\tilde{h}_1(r_{Ds},z_D,p)}{\partial r_D}=\gamma\frac{\partial\tilde{h}_2(r_{Ds},z_D,p)}{\partial r_D} \tag{27}$$

$$\frac{\partial\tilde{h}_1(r_D,0,p)}{\partial z_D}=\frac{\partial\tilde{h}_2(r_D,0,p)}{\partial z_D}=0 \tag{28}$$

$$\frac{\partial\tilde{h}_1(r_D,L_D,p)}{\partial z_D}=\frac{\partial\tilde{h}_2(r_D,L_D,p)}{\partial z_D}=0 \tag{29}$$

$$\tilde{h}_1(1,z_D,p)=\frac{1}{p} \tag{30}$$

$$-\frac{\partial\tilde{h}_1(1,z_D,p)}{\partial r_D}=q_D(p),\quad b_1\leq z_D\leq b_2 \tag{31}$$

and

$$-\frac{\partial\tilde{h}_1(1,z_D,p)}{\partial r_D}=0,\quad z_D<b_1,\quad z_D>b_2 \tag{32}$$

Applying the finite Fourier cosine and inverse finite Fourier cosine transforms with respect to the z coordinate for Eqs. (23)–(32) results in dimensionless hydraulic heads for the skin and formation zones, respectively,

$$\tilde{h}_1=\tilde{q}_D(p)\left[\phi A_1(r_D)+\frac{2}{L_D}\sum_{n=1}^{\infty}A_2(r_D)A_3(w_n)\cos(w_nz_D)\right] \tag{33}$$

and

$$\tilde{h}_2=\tilde{q}_D(p)\left[\phi B_1(r_D)+\frac{2}{L_Dr_{Ds}}\sum_{n=1}^{\infty}B_2(r_D)A_3(w_n)\cos(w_nz_D)\right] \tag{34}$$

where

$$A_1(r_D)=\frac{[-\beta_3I_0(q_3r_D)+\beta_4K_0(q_3r_D)]}{q_3[\beta_3I_1(q_3)+\beta_4K_1(q_3)]} \tag{35}$$

$$A_2(r_D)=\frac{[-\beta_1I_0(q_1r_D)+\beta_2K_0(q_1r_D)]}{q_1[\beta_1I_1(q_1)+\beta_2K_1(q_1)]} \tag{36}$$

J. Hydraul. Eng. 2005.131:209-216.

$$A_3(w_n) = \frac{[\sin(w_n b_2) - \sin(w_n b_1)]}{w_n} \tag{37}$$

$$B_1(r_D) = \frac{K_0(q_4 r_D)}{q_3 r_{Ds}[\beta_3 I_1(q_3) + \beta_4 K_1(q_3)]} \tag{38}$$

and

$$B_2(r_D) = \frac{K_0(q_2 r_D)}{q_1 r_{Ds}[\beta_1 I_1(q_1) + \beta_2 K_1(q_1)]} \tag{39}$$

where p=Laplace variable (Spiegel 1965); $w_n = n\pi/L_D$; and $\tilde{q}_D(p)$=dimensionless flow rate in the Laplace domain. The functions of $I_0(\cdot)$ and $K_0(\cdot)$ are, respectively, the modified Bessel functions of the first and second kinds of order zero; and $I_1(\cdot)$ and $K_1(\cdot)$ are the modified Bessel functions of the first and second kinds of order one, respectively. Note that the dimensionless flow rate $\tilde{q}_D(p)$ in Eq. (33) is unknown and can be obtained by substituting Eq. (33) into Eq. (30) as

$$\tilde{q}_D(p) = \frac{1}{p}\left[\phi A_1(r_D = 1) + \frac{2}{L_D(b_2 - b_1)}\sum_{n=1}^{\infty} A_2(r_D = 1)A_3^2(w_n)\right]^{-1} \tag{40}$$

This equation has two terms; the first term accounts for the behavior of a fully penetrating well and the second term is associated with the effect of well partial penetration.

Proof of the Solution

This section proves that the Laplace-domain solutions of dimensionless hydraulic heads satisfy the governing equations, boundary conditions, and continuity requirements at the interface of the skin zone and undisturbed formation. McLachlan (1955, pp. 192–197) gave following two formulas:

$$\frac{\partial I_0(qr_D)}{\partial r_D} = qI_1(qr_D) \tag{41}$$

and

$$\frac{\partial^2 I_0(qr_D)}{\partial r_D^2} = q^2\left[-\frac{1}{qr_D}I_1(qr_D) + I_0(qr_D)\right] \tag{42}$$

Based on Eqs. (41) and (42), one can obtain

$$\frac{\partial^2 I_0(qr_D)}{\partial r_D^2} + \frac{1}{r_D}\frac{\partial I_0(qr_D)}{\partial r_D} = q^2 I_0(qr_D) \tag{43}$$

Similarly,

$$\frac{\partial^2 K_0(qr_D)}{\partial r_D^2} + \frac{1}{r_D}\frac{\partial K_0(qr_D)}{\partial r_D} = q^2 K_0(qr_D) \tag{44}$$

Based on Eqs. (35), (43), and (44), the sum of the second derivative of $A_1(r_D)$ with respect to r_D and the first derivative of $A_1(r_D)$ with respect to r_D divided by r_D gives

$$\frac{\partial^2 A_1(r_D)}{\partial r_D^2} + \frac{1}{r_D}\frac{\partial A_1(r_D)}{\partial r_D} = \frac{\left\{-\beta_3\left[\frac{\partial^2 I_0(q_3 r_D)}{\partial r_D^2} + \frac{1}{r}\frac{\partial I_0(q_3 r_D)}{\partial r_D}\right] + \beta_4\left[\frac{\partial^2 K_0(q_3 r_D)}{\partial r_D^2} + \frac{1}{r}\frac{\partial K_0(q_3 r_D)}{\partial r_D}\right]\right\}}{q_3[\beta_3 I_1(q_3) + \beta_4 K_1(q_3)]} = q_3^2 A_1(r_D) \tag{45}$$

Likewise, one can get

$$\frac{\partial^2 A_2(r_D)}{\partial r_D^2} + \frac{1}{r_D}\frac{\partial A_2(r_D)}{\partial r_D} = q_1^2 A_2(r_D) \tag{46}$$

Substituting $\tilde{h}_1$ of Eq. (33) into the left-hand side (LHS) of Eq. (23) and using Eqs. (45) and (46) yields

$$\tilde{q}_D(p)\left[\phi\left[\frac{\partial^2 A_1(r_D)}{\partial r_D^2} + \frac{1}{r_D}\frac{\partial A_1(r_D)}{\partial r_D}\right] + \frac{2}{L_D}\sum_{n=1}^{\infty}\left[\frac{\partial^2 A_2(r_D)}{\partial r_D^2} + \frac{1}{r_D}\frac{\partial A_2(r_D)}{\partial r_D}\right]A_3(w_n)\cos(w_n z_D)\right] = \gamma\xi p\tilde{h}_1 \tag{47}$$

Here, we have shown that the solution for dimensionless head distribution in the skin zone, Eq. (33), satisfies the governing equation (23). Also, one can prove that Eq. (34) satisfies the governing equation (24).

For the outer boundary, $r_D \to \infty$, one has $K_0(\infty) = 0$ and $K_1(\infty) = 0$; accordingly, $B_1(\infty)$ and $B_2(\infty)$ in Eqs. (38) and (39) equal zero. The dimensionless hydraulic head of Eq. (34) is then equal to zero when $r_D \to \infty$. Therefore, Eq. (34) satisfies the outer boundary condition of Eq. (25).

Letting $r_D = r_{Ds}$ and using the dimensionless expression for β_3 and β_4, Eq. (35) equals

$$A_1(r_{Ds}) = \frac{1}{q_3[\beta_3 I_1(q_3) + \beta_4 K_1(q_3)]} \times \{q_3 K_0(q_4 r_{Ds})[K_1(q_3 r_{Ds})I_0(q_3 r_{Ds}) + I_1(q_3 r_{Ds})K_0(q_3 r_{Ds})]\} \tag{48}$$

Based on the formula $K_1(u)I_0(u) + I_0(u)K_1(u) = 1/u$ (Abramowitz and Stegun 1964) and Eq. (38), Eq. (48) reduces to $A_1(r_{Ds}) = B_1(r_{Ds})$. Similarly, $A_2(r_{Ds}) = B_2(r_{Ds})$. As a result, Eq. (33) is equal to Eq. (34) at $r_D = r_{Ds}$. Here, we have shown the continuity of dimensionless hydraulic head between the skin and formation zones.

Taking the derivative of $A_1(r_D)$ in Eq. (35) with respect to r_D and letting $r_D = r_{Ds}$ produces

$$\left.\frac{\partial A_1(r_D)}{\partial r_D}\right|_{r_D = r_{Ds}} = \frac{-\gamma q_4 K_1(q_4 r_{Ds})}{q_3 r_{Ds}[\beta_3 I_1(q_3) + \beta_4 K_1(q_3)]} \tag{49}$$

Also,

$$\left.\frac{\partial A_2(r_D)}{\partial r_D}\right|_{r_D = r_{Ds}} = \frac{-\gamma q_2 K_1(q_2 r_{Ds})}{q_1 r_{Ds}[\beta_1 I_1(q_1) + \beta_2 K_1(q_1)]} \tag{50}$$

J. Hydraul. Eng. 2005.131:209-216.

Furthermore, letting $r_D = r_{Ds}$ and multiplying by γ on both sides after taking the derivative of $B_1(r_D)$ in Eq. (38) with respect to r_D yields

$$\gamma \left.\frac{\partial B_1(r_D)}{\partial r_D}\right|_{r_D=r_{Ds}} = \frac{-\gamma q_4 K_1(q_4 r_{Ds})}{q_3 r_{Ds}[\beta_3 I_1(q_3) + \beta_4 K_1(q_3)]} \tag{51}$$

Likewise,

$$\gamma \left.\frac{\partial B_2(r_D)}{\partial r_D}\right|_{r_D=r_{Ds}} = \frac{-\gamma q_2 K_1(q_2 r_{Ds})}{q_1 r_{Ds}[\beta_1 I_1(q_1) + \beta_2 K_1(q_1)]} \tag{52}$$

Therefore, based on Eqs. (49)–(52), one can easily prove that

$$\left.\frac{\partial \tilde{h}_1}{\partial r_D}\right|_{r_D=r_{Ds}} = \gamma \left.\frac{\partial \tilde{h}_2}{\partial r_D}\right|_{r_D=r_{Ds}} \tag{53}$$

Here, we have shown that the flow rates between the skin and formation zones are equal.

The derivatives of the hydraulic heads in Eqs. (33) and (34) with respect to z_D produce sine terms and become zero when z_D equals 0 or L_D. Thus, the no-flow condition at the top and bottom boundaries, Eqs. (28) and (29), is satisfied.

Simplified Solutions

The Laplace-domain solutions for dimensionless head distribution in the skin and formation zones, i.e., Eqs. (33) and (34), and dimensionless flow rate cross the wellbore, Eq. (40), can reduce to a simpler form if the aquifer is homogeneous or/and the well is fully penetrating.

Homogeneous Aquifer

For the case of a partially penetrating well in a homogeneous (single zone) aquifer, both γ and ξ are equal to unity and $\alpha_1 = \alpha_2 = 1$. Let the variables q_1 and q_2 equal dummy variable q and q_3 and q_4 equal dummy variable q'; consequently, both β_1 and β_3 become zero. Then, Eqs. (35) and (38) turn out to be

$$C_1(r_D) = A_1(r_D) = B_1(r_D) = \frac{K_0(q' r_D)}{q' K_1(q')} \tag{54}$$

and Eqs. (36) and (39) become

$$C_2(r_D) = A_2(r_D) = B_2(r_D) = \frac{K_0(q r_D)}{q K_1(q)} \tag{55}$$

Then, the dimensionless hydraulic heads for the skin and formation zones, Eqs. (33) and (34), reduce to the solution for a homogeneous aquifer as

$$\tilde{h}_1 = \tilde{q}_D(p)\left[\phi C_1(r_D) + \frac{2}{L_D}\sum_{n=1}^{\infty} C_2(r_D) A_3(w_n)\cos(w_n z_D)\right] \tag{56}$$

and the equation representing dimensionless flow rate, Eq. (40), turns into

$$\tilde{q}_D(p) = \frac{1}{p}\left[\phi C_1(r_D = 1) + \frac{2}{L_D(b_2 - b_1)}\sum_{n=1}^{\infty} C_2(r_D = 1) A_3^2(w_n)\right]^{-1} \tag{57}$$

Fully Penetrating Well

For a fully penetrating well case, by setting $b_1 = 0$ and $b_2 = L_D$, one can obtain $\phi = 1$ and $A_3(w_n) = 0$. Consequently, those terms with a summation on the right-hand side of Eqs. (33), (34), and (40) are all equal to zero. Thus, the dimensionless hydraulic heads in the skin and formation zones are, respectively,

$$\tilde{h}_1 = \frac{1}{p}\frac{[-\beta_3 I_0(q_3 r_D) + \beta_4 K_0(q_3 r_D)]}{[-\beta_3 I_0(q_3) + \beta_4 K_0(q_3)]} \tag{58}$$

and

$$\tilde{h}_2 = \frac{1}{p}\frac{K_0(q_4 r_D)}{r_{Ds}[-\beta_3 I_0(q_3) + \beta_4 K_0(q_3)]} \tag{59}$$

and the dimensionless flow rate is

$$\tilde{q}_D = \frac{1}{p}\frac{q_3[\beta_3 I_1(q_3) + \beta_4 K_1(q_3)]}{[-\beta_3 I_0(q_3) + \beta_4 K_0(q_3)]} \tag{60}$$

which indeed are equal to those Laplace-domain solutions for the dimensionless head distribution and wellbore flux for a two-zone aquifer system presented in Yang and Yeh (2002). With some minor algebraic manipulations, Eq. (60) is the equivalent to Eq. (14) of Novakowski (1993).

Homogeneous Aquifer and Fully Penetrating Well

For a homogeneous aquifer, the skin is absent and the aquifer properties are constant throughout the whole aquifer. Accordingly, both γ and ξ are equal to unity and let the variables q_3 and q_4 in Eqs. (58)–(60) also equal the dummy variable q'. Then, both, Eqs. (58) and (59) reduce to

$$\tilde{h}_D = \frac{1}{p}\frac{K_0(q' r_D)}{K_0(q')} \tag{61}$$

and Eq. (60) becomes

$$\tilde{q}_D(p) = \frac{K_1(q')}{\sqrt{p} K_0(q')} \tag{62}$$

which are the Laplace-domain solutions, respectively, for dimensionless head distribution in the aquifer and dimensionless flow rate at the wellbore presented in Carslaw and Jaeger (1939) and Jaeger (1942).

Results and Discussion

Note that Eqs. (33) and (34), respectively, stand for dimensionless hydraulic heads in the skin and formation zones and Eq. (40) represents the dimensionless flow rate at the wellbore. These equations consist of the products of the Bessel functions which can be approximated by the formulas given in Abramowitz and Stegun (1964) and Watson (1958). Since Bessel functions are oscillatory function and may be slowly convergent in certain cases, the evaluations of these functions are accelerated using the Shanks method (Shanks 1955; Yang and Yeh 2002). The values of the Bessel functions in these equations are computed at least to ten decimal places, and thus have the same accuracy as those listed in Abramowitz and Stegun (1964) and Watson (1958). The routine INLAP of IMSL (1987) developed based on the modified Crump method (Crump 1976; de Hoog et al. 1982) is employed to

J. Hydraul. Eng. 2005.131:209-216.

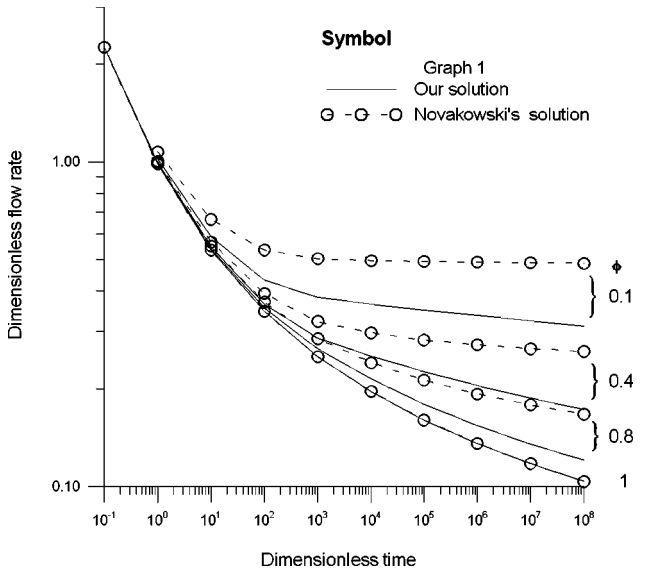

Fig. 2. Relationship for dimensionless flow rate against dimensionless time for $\gamma=1$ (no skin) and $L_D=200$ when $\phi=0.1$, 0.4, 0.8, or 1.0

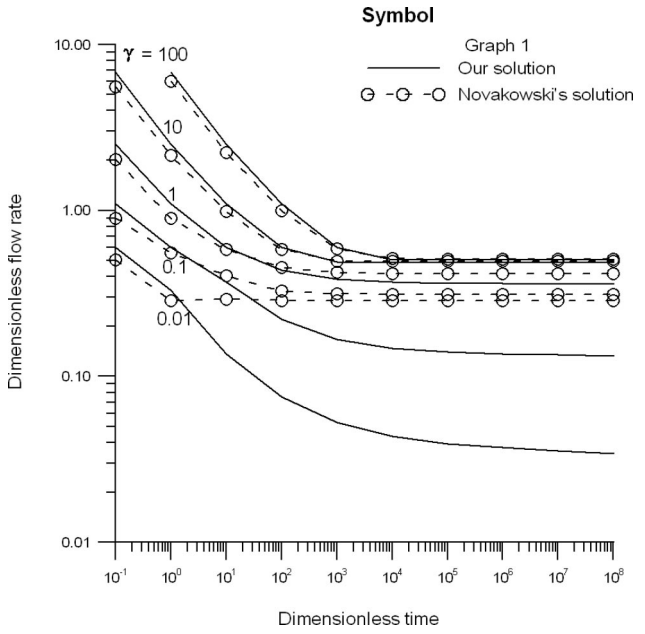

Fig. 3. Relationship for dimensionless flow rate against dimensionless time for $L_D=2000$, $r_{Ds}=10$, and $\phi=0.01$ when $\gamma=0.01$, 0.1, 1 (no skin), 10, or 100

invert those Laplace-domain solutions numerically. This method approximates the Laplace inversion by expressing the transformed function in a Fourier series.

Comparisons of Our Solution and Novakowski's Solution for Dimensionless Flow Rate

The curves of dimensionless flow rate versus dimensionless time are plotted to investigate the impacts of the skin properties and thickness on dimensionless flow rate. For ease of comparison, ξ, α_1, and α_2 are chosen as one. In addition, all evaluations for the solution are in a double-precision format. Note that the aquifer has a negative skin when the conductivity ratio $\gamma<1$ and a positive skin when $\gamma>1$; on the other hand, the two-zone aquifer system becomes a uniform (single-zone) medium when $\gamma=1$.

For $\gamma=1$ (no skin) and $L_D=200$ (dimensionless aquifer thickness) when ϕ (dimensionless screen length)$=0.1$, 0.4, 0.8, or 1, Fig. 2 depicts the relationship for dimensionless flow rate against dimensionless time. Note that $\phi=1$ represents a fully penetrating well case. The dimensionless flow rate tends to decrease rapidly with increasing dimensionless time and stabilizes when dimensionless time is very large. The dimensionless flow rate with a partially penetrating well significantly differs from that with a fully penetrating well. The dimensionless flow rate increases with decreasing ϕ at the same dimensionless time. A larger dimensionless flow rate reflects the effect of screen length. Obviously, a smaller screen length will have a larger dimensionless flow rate for a constant-head test. The effect of well partial penetration increases with dimensionless time. Fig. 2 also displays the comparisons between our solution and Novakowski's solution when the finite-thickness skin is absent. The dimensionless flow rates of our solution match with those of Novakowski's solution when $\phi=1$. However, dimensionless flow rates of Novakowski's solution are significantly larger than those of our solution when $\phi<1$. In addition, the differences between our solution and Novakowski's solution increase with increasing dimensionless time and decreasing ϕ.

For $L_D=2000$, $r_{Ds}=10$, and $\phi=0.01$ when $\gamma=0.01$, 0.1, 1 (no skin), 10, or 100, Fig. 3 shows the relationship of dimensionless flow rate versus dimensionless time. The dimensionless flow rate decreases rapidly with increasing dimensionless time and stabilizes when dimensionless time is very large (say, $\tau>10^3$). The dimensionless flow rate increases with γ at the same dimensionless time. A larger dimensionless flow rate reflects the effect of the conductivity ratio, γ. Fig. 3 also displays the comparison between our solution and Novakowski's solution on the effects of finite-thickness skin and well partial penetration. The dimensionless flow rates calculated based on Novakowski's solution are smaller than those of our solution at early dimensionless time and larger at late dimensionless time, especially for small value of γ. The curves of dimensionless flow rate versus dimensionless time drawn based on Novakowski's solution for the well with a negative skin becomes flat when dimensionless time is small. This problem may also be attributed to the assumption of using the constant-head condition for the casing in his mathematical model.

Effect of Finite-Thickness Skin on Dimensionless Hydraulic Head

Fig. 4 displays the plot of dimensionless hydraulic head versus dimensionless distance for $L_D=200$, $r_{Ds}=10$, $z_D=100$, $\phi=0.1$, and $\tau=10^2$, 10^4, 10^6, and 10^8 when $\gamma=0.1$, 1, or 10. This figure demonstrates the effect of skin properties on the shape of curves in a partially penetrating well. The dimensionless hydraulic head increases with dimensionless time in both the skin and formation zones; contrarily, the dimensionless hydraulic head decreases with increasing dimensionless radial distance. For the case without a skin zone ($\gamma=1$), dimensionless head gradually decreases when increasing radial distance. At the interface of the skin and formation zones (i.e., $r_D=r_{Ds}$), the slopes of curves are markedly different because of the contrast of hydraulic conductivity between skin and formation zones. Under negative skin condition, the slope of curve within the skin zone is obviously smaller than that within formation zone due to the fact of larger hydraulic conductivity of the negative skin. In contrast, the slope of curve

J. Hydraul. Eng. 2005.131:209-216.

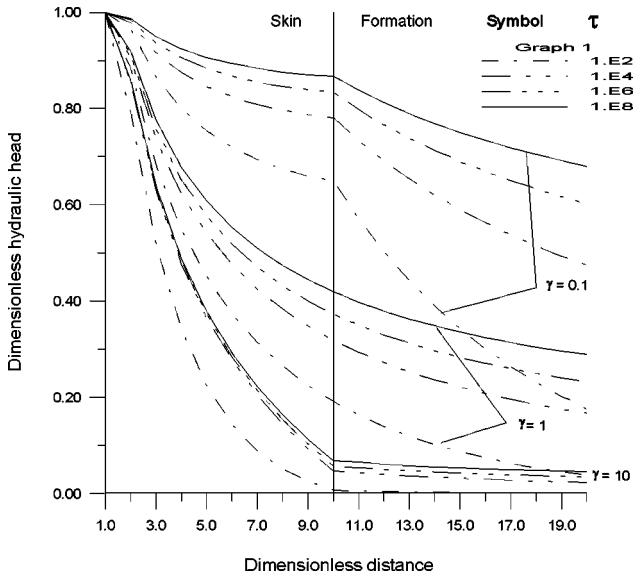

Fig. 4. Plot of dimensionless hydraulic head versus dimensionless distance for $L_D=200$, $r_{Ds}=10$, $z_D=100$, $\phi=0.1$, and $\tau=10^2$, 10^4, 10^6, and 10^8 when $\gamma=0.1$, 1, or 10

within the skin zone is larger than that within the formation zone under positive skin condition. For a larger dimensionless distance, the curves become flat and parallel. Obviously, the presence of skin influences the hydraulic head distribution in aquifers for constant-head tests with a partially penetrating well.

Fig. 5 exhibits the curves of dimensionless hydraulic head versus dimensionless time for $L_D=200$, $r_{Ds}=10$, $z_D=100$, $\phi=0.1$, and $r_D=5$, 10, and 15 when $\gamma=0.1$, 1, or 10. At $r_D=5$, 10, and 15, the negative skin ($\gamma=0.1$) produces the highest dimensionless hydraulic head, the no skin ($\gamma=1$) gives the second, and the positive skin ($\gamma=10$) yields the lowest under the same dimensionless time. Larger hydraulic conductivity of a negative skin produces a larger flow rate toward the undisturbed formation during the well test

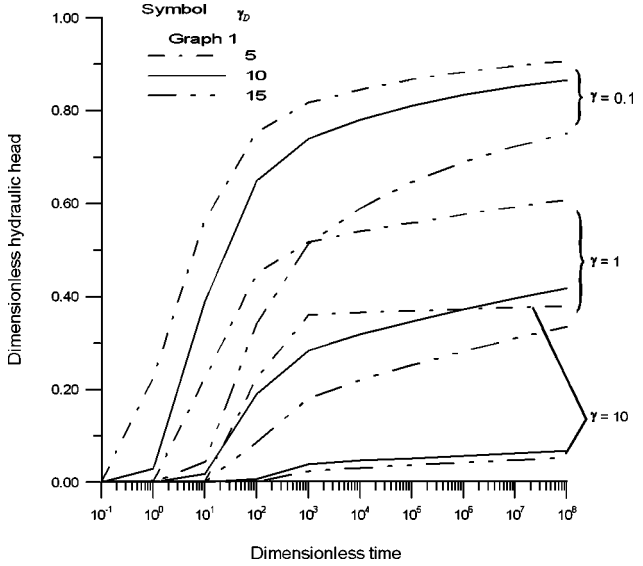

Fig. 5. Effect of skin properties on the shape of curves for $L_D=200$, $r_{Ds}=10$, $z_D=100$, $\phi=0.1$, and $r_D=5$, 10, and 15 when $\gamma=0.1$, 1, or 10

and results in a higher dimensionless hydraulic head. On the other hand, a lower hydraulic conductivity of a positive skin yields a lower flow rate at the wellbore and results in smaller dimensionless heads of the skin and formation zones.

Conclusions

A mathematical model is presented for a constant-head test performed in a well under the effects of the finite-thickness skin and well partial penetration. The model uses a no-flow boundary condition for the casing and constant-head boundary condition for the screen to represent a partially penetrating well. Laplace-domain solutions for both the dimensionless flow rate at the wellbore and the hydraulic heads in the skin and formation zones are derived using the Laplace and finite Fourier cosine transforms. The solutions of hydraulic heads have been shown to satisfy the governing equations, related boundary conditions, and continuity requirements for the hydraulic head and flow rate at the interface of the skin zone and undisturbed formation. In addition, simplified solutions for the cases of homogenous aquifer and/or fully penetrating well are also given. An efficient algorithm for evaluating this new solution is also presented. The algorithm includes the modified Crump method for performing the numerical Laplace inversion and the Shanks method for accelerating convergence when evaluating the sum of terms and the Bessel functions.

For the case with a fully penetrating well and finite-thickness skin, the dimensionless flow rates computed from our solution agree with those of Novakowski's solution. However, under a partially penetrating condition, the dimensionless flow rates evaluated based on our solution and Novakowski's solution are significantly different, especially when $\gamma<1$ and $\tau>1$. This problem may be due to the fact that Novakowski assumed the hydraulic head to be constant even in the portion of well casing in his mathematical model. The curve for the dimensionless head distribution shows an abrupt change in slope at the interface between the skin and formation zones. The shape of dimensionless hydraulic head distribution is affected substantially when the finite-thickness skin presents. For a two-zone aquifer system, our solutions can be used for predicting the hydraulic head distributions and the transient flow rate at the wellbore, exploring the effects of the finite-thickness skin and well partial penetration on either the hydraulic heads or the transient flow rate, and identifying the aquifer parameters via aquifer tests and data analyses.

Acknowledgments

The writers appreciate the comments and suggested revisions of two anonymous reviewers that help improve the clarity of our presentation. Research leading to this paper has been partially supported by Taiwan National Science Council under Grant No. NSC91-2211-E-009-020 and Taiwan Van-Nung Institute of Technology under Contract No. VIT-92-CE-003.

References

Abramowitz, M., and Stegun, I. A. (1964). *Handbook of mathematical functions with formulas, graphs and mathematical tables*, National Bureau of Standards, Washington, Dover, New York.

Carslaw, H. S., and Jaeger, J. C. (1939). "Some two-dimensional problems in conduction of heat with circular symmetry." *Some problems*

in conduction of heat, Vol. 46, 361–388.
Cassiani, G., Kabala, Z. J., and Medina, M. A., Jr., (1999). "Flowing partially penetrating well: solution to a mixed- type boundary value problem." *Adv. Water Resour.*, 23, 59–68.
Chang, C. C., and Chen, C. S. (1999). "Analysis of constant-head for a two-layer radially symmetric nonuniform model." *Proc., 3rd Groundwater Resources and Water Quality Protection Conference*, National Central Univ., Chung-Li, Taiwan.
Chang, C. C., and Chen, C. S. (2002). "An integral transform approach for a mixed boundary problem involving a flowing partially penetrating well with infinitesimal well skin." *Water Resour. Res.*, 38(6), 7-1–7-7.
Crump, K. S. (1976). "Numerical inversion of Laplace transforms using a Fourier series approximation." *J. Assoc. Comput. Mach.*, 23(1), 89–96.
de Hoog, F. R., Knight, J. H., and Stokes, A. N. (1982). "An improved method for numerical inversion of Laplace transforms." *SIAM (Soc. Ind. Appl. Math.) J. Sci. Stat. Comput.*, 3(3), 357–366.
International Mathematics and Statistics Library Inc. (IMSL). (1987). *IMSL user's manual*, Vol. 2, IMSL, Inc., Houston.
Jaeger, J. C. (1942). "Heat flow in the region bounded internally by a circular cylinder." *Proc. R. Soc. Edinburgh, Sect. A: Math. Phys. Sci.*, 61, 223–228.
Markle, J. M., Rowe, R. K., and Novakowski, K. S. (1995). "A model for the constant-head pumping test conducted in vertically fractured media." *Int. J. Numer. Analyt. Meth. Geomech.*, 19, 457–473.
McLachlan, N. W. (1955). *Bessel functions for engineers*, 2nd Ed., Oxford University Press, London.
Novakowski, K. S. (1989). "A composite analytical model for analysis of pumping tests affected by wellbore storage and finite thickness skin." *Water Resour. Res.*, 25(9), 1937–1946.
Novakowski, K. S. (1993). "Interpretation of the transient flow rate obtained from constant-head tests conducted in situ in clays." *Can. Geotech. J.*, 30, 600–606.
Shanks, D. (1955). "Nonlinear transformations of divergent and slowly convergent sequences." *J. Math. Phys. (Cambridge, Mass.)*, 34, 1–42.
Spiegel, M. R. (1965). *Laplace transforms*, Schaum, New York.
Streltsova, T. D., and McKinley, R. M. (1984). "Effect of flow time duration on buildup pattern for reservoirs with heterogeneous properties." *Soc. Pet. Eng. J.*, 294–306.
Watson, G. N. (1958). *A treatise on the theory of bessel functions*, 2nd Ed., Cambridge University Press, Cambridge, U.K.
Yang, S. Y., and Yeh, H. D. (2002). "Solution for flow rates across the wellbore in a two-zone confined aquifer." *J. Hydraul. Eng.*, 128(2), 175–183.

J. Hydraul. Eng. 2005.131:209-216.